Inorg. Chem. **2005**, *44*, 4522–4533

^{1}H NMR Investigation of High-Spin and Low-Spin Iron(III) *meso*-Ethynylporphyrins

Anna Berlicka, Lechosław Latos-Grażyński,* and Tadeusz Lis

Department of Chemistry, University of Wrocław, 50 383 Wrocław, Poland

Received January 31, 2005

The ^{1}H NMR spectra of iron(III) 5-ethynyl-10,15,20-tri(*p*-tolyl)porphyrin [(ETrTP)Fe^{III}X$_n$], iron(III) 5-(phenylethynyl)-10,15,20-tri(*p*-tolyl)porphyrin [(PETrTP)Fe^{III}X$_n$], iron(III) 5-(phenylbutadiynyl)-10,15,20-tri(*p*-tolyl)porphyrin [(PBTrTP)-Fe^{III}X$_n$], iron(III) 5,10,15,20-tetra(phenylethynyl)porphyrin [(TPEP)Fe^{III}X$_n$], iron(III) 1,4-bis-[10,15,20-tri(*p*-tolyl)porphyrin-5-yl]-1,3-butadiyne {[(TrTP)Fe^{III}X$_n$]$_2$B}, and 5,10,15-triphenylporphyrin [(TrPP)Fe^{III}X$_n$] have been studied to elucidate the impact of *meso*-ethynyl substitution on the electronic structure and spin density distribution of high-spin (X = Cl$^-$, n = 1) and low-spin (X = CN$^-$, n = 2) derivatives. The meso substituents, i.e., ethynyl, phenylethynyl, and phenylbutadiynyl, provided insight into the efficiency of spin density delocalization along structural elements that are typically applied to transmit electronic effects along multipart polyporphyrinic systems. The positive spin density localized at the *meso*-carbon of high-spin iron(III) ethynylporphyrins is effectively delocalized along the ethyne or butadiyne fragment as illustrated by the comparison of isotropic shifts of C_{meso}–**H** and –CC–**H** determined for (TrPP)Fe^{III}Cl (–82.6 ppm, 293 K) and (ETrTP)Fe^{III}Cl (–49.5 ppm, 298 K). The replacement of the ethynyl hydrogen by phenyl or phenylethynyl provided evidence for the π spin density distribution around the introduced phenyl ring. An analysis of the isotropic shifts for the low-spin bis-cyanide iron(III) porphyrins series reveals the analogous mechanism of spin density transfer. Treatment of high-spin [(TrTP)Fe^{III}Cl]$_2$B with a base resulted in formation of the cyclic [(TrTP)Fe^{III}OFe^{III}(TrTP)B]$_2$ complex linked by two μ-oxo bridges. (TPEP)H$_2$ has been characterized by X-ray crystallography as a porphyrin dication where two molecules of trifluoroacetic acid associate with two coordinated trifluoroacetate anions. The X-ray structure of bis-tetrahydrofuran 1,4-bis[10,15,20-tri(*p*-tolyl)porphyrinatozinc(II)-5-yl]-1,3-butadiyne complex {[(TrTP)Zn^{II}(THF)]$_2$B} reveals two parallel, non-coplanar [(TrTP)Zn(THF)] subunits linked by the linear butadiyne moiety.

Introduction

The electronic structure of iron porphyrins represents a continuously active and challenging area of research, especially because of the relevance of such studies to the structure and function of catalytic systems based on hemoproteins and iron porphyrins. In this line of investigations, ^{1}H NMR spectroscopy provides a particularly useful tool for characterizing the oxidation/spin/ligation states of paramagnetic hemoproteins and iron porphyrins.[1−4] The interaction with unpaired spin(s) at the metal ion induces large hyperfine shifts for the substituent protons of iron porphyrins, and this allows unambiguous assignments of the electronic structure based on characteristic hyperfine shift patterns for various functional groups. The hyperfine shift pattern is distinct for each oxidation/spin/ligation state of iron porphyrins.

Several modifications of iron porphyrins that allow fine-tuning of electronic properties including the spin density distribution have been explored. For instance, the spin density distribution in iron(III) porphyrins can be controlled by the following molecular features: controlled substitution at the 3 and 8 positions of deuterioporphyrin;[5] the nature of the substituents and the pattern of their distribution in iron(III)

* To whom correspondence should be addressed. E-mail: LLG@wchuwr.chem.uni.wroc.pl.

(1) Walker, F. A. Proton NMR and EPR Spectroscopy of Paramagnetic Metalloporphyrins. In *The Porphyrin Handbook*; Kadish, K. M., Smith, K. M., Guilard, R., Eds.; Academic Press: San Diego, CA, 2000; pp 81−183.

(2) Walker, F. A. *Inorg. Chem.* **2003**, *42*, 4526.

(3) Banci, L.; Bertini, I.; Luchinat, C.; Turano, P. Solutions Sturctures of Hemoproteins. In *The Porphyrin Handbook*; Kadish, K. M., Smith, K. M., Guilard, R., Eds.; Academic Press: San Diego, CA, 2000; pp 323−350.

(4) La Mar, G. N.; Satterlee, J. D.; De Ropp, J. S. Nuclear Magnetic Resonance of Hemoproteins. In *The Porphyrin Handbook*; Kadish, K. M., Smith, K. M., Guilard, R., Eds.; Academic Press: San Diego, CA, 2000; pp 185−298.

10.1021/ic050158q CCC: $30.25
Published on Web 05/28/2005

octa-β-substituted porphyrin isomers;[6] monosubstitution of the β-pyrrole position of tetraphenylporphyrins;[7] meso substitution of 5,10,15-triphenylporphyrin;[8] substitution of the *meso*-phenyl ring(s) in iron(III) tetraphenylporphyrins;[1,9] saturation of pyrrole rings to form iron(III) chlorins, sulfhemins, or dioxoisobacteriochlorin;[10−12] the mutual orientation of planar nitrogen bases coordinated in axial positions;[13] and the π-acceptor character of the axial ligand.[14] Recent studies have documented that the replacement of *meso*-aryl substituents of extensively investigated 5,10,15,20-tetrarylporphyrins by alkyl groups profoundly influences the molecular and electronic structures of iron(III) porphyrins.[15−18]

Apart from perimeter substitution, a fundamentally different approach involving core alteration has been suggested as an independent route for control of the iron porphyrin electronic and molecular structure.[19−21] The specific properties of iron porphyrin isomers have provided noteworthy insight into properties of iron porphyrins as well.[22−26]

Here, in the search for suitable means to control electronic structures and spectroscopic properties of iron(III) porphyrins, we have decided to probe a distinctive class of meso-substituted porphyrins, namely, ethynylporphyrins. Ethynylporphyrins have at least one *meso*-carbon directly linked to the ethynyl group.[27] The ethynyl substituent—because of its linear geometry—is expected to generate minimal steric hindrance, which might favor an overall planar geometry of the macrocycle. The electronic structure of the ethynyl(s) allows the extensive conjugation with the porphyrinic macrocycle readily accounting for the general features of alkynyl porphyrins, which include significantly red-shifted absorption spectra and less negative reduction potentials.[27]

The investigation of ethynylporphyrins originated with the synthesis of nickel(II) octaethylporphyrin bearing the ethynyl group at the meso position.[28] Further synthetic studies yielded tetraethynyl-substituted porphyrins.[29−31] Eventually, porphyrins bearing arylethynyl substituents at four meso positions were synthesized.[32,33] The arylethynyl moieties allow the electronic structure to be tuned and the solubility of the porphyrin to be increased,[32−37] as readily illustrated by the fact that 5,10,15,20-tetra(phenylethynyl)porphyrin (common name chlorphyrin) yields, untypical for meso-substituted porphyrins, a green solution.[32] Ethynyl- or butadiynyl-linked multiporphyrin arrays have also been synthesized and characterized.[38−41] Such compounds belong to the larger class of multiporphyrins that have been explored as light-harvesting antennas and charge-separation devices for studies in artificial photosynthesis.[42−44]

In this Article, we study the impact of the meso substitution of iron(III) porphyrin by ethynyl moiety(ies) on the ^{1}H NMR properties. Representative examples of the ethynylporphyrin class, namely, 5-ethynyl-10,15,20-tri(*p*-tolyl)porphyrin (**1**), 5-(phenylethynyl)-10,15,20-tri(*p*-tolyl)porphyrin (**2**), 5-(phenylbutadiynyl)-10,15,20-tri(*p*-tolyl)porphyrin (**3**), 5,-10,15,20-tetra(phenylethynyl)porphyrin (**4**), and 1,4-bis-[10,-15,20-tri(*p*-tolyl)porphyrin-5-yl]-1,3-butadiyne (**5**), were chosen for these investigations (Chart 1). The resonances of the pyrrole hydrogens provide a direct probe of the electronic structure and spin density around the porphyrin macrocycle. The transfer of the spin density along ethyne and butadiyne linkers has been of the special interest. These structural

(5) La Mar, G. N.; Viscio, D. B.; Smith, K. M.; Caughey, W. S.; Smith, M. L. *J. Am. Chem. Soc.* **1978**, *100*, 8085.
(6) Isaac, M. F.; Lin, Q.; Simonis, U.; Suffian, D. J.; Wilson, D. L.; Walker, F. A. *Inorg. Chem.* **1993**, *32*, 4030.
(7) Wojaczyński, J.; Latos-Grażyński, L.; Hrycyk, W.; Pacholska, E.; Rachlewicz, K.; Szterenberg, L. *Inorg. Chem.* **1996**, *35*, 6861.
(8) Wojaczyński, J.; Stępień, M.; Latos-Grażyński, L. *Eur. J. Inorg. Chem.* **2002**, *7*, 1806.
(9) Walker, F. A.; Balke, V. L.; McDermott, G. A. *J. Am. Chem. Soc.* **1982**, *104*, 1569.
(10) Chatfield, M. J.; La Mar, G. N.; Parker, W. O.; Smith, K. M.; Leung, H. K.; Morris, I. K. *J. Am. Chem. Soc.* **1988**, *110*, 6352.
(11) Liccocia, S.; Chatfield, M. J.; La Mar, G. N.; Smith, K. M.; Mansfield, K. E.; Anderson, R. R. *J. Am. Chem. Soc.* **1989**, *111*, 6087.
(12) Barkigia, K. M.; Chang, C. K.; Fajer, J.; Renner, M. W. *J. Am. Chem. Soc.* **1992**, *114*, 1701.
(13) Walker, F. A.; Simonis, U. *J. Am. Chem. Soc.* **1991**, *113*, 8652.
(14) Simonneaux, G.; Schunemann, V.; Morice, C.; Carel, L.; Toupet, L.; Winkler, H.; Trautwein, A. X.; Walker, F. A. *J. Am. Chem. Soc.* **2000**, *122*, 4366.
(15) Wołowiec, S.; Latos-Grażyński, L.; Mazzanti, M.; Marchon, J.-C. *Inorg. Chem.* **1997**, *36*, 5761.
(16) Mazzanti, M.; Marchon, J.-C.; Wojaczyński, J.; Wołowiec, S.; Latos-Grażyński, L.; Shang, M.; Scheidt, W. R. *Inorg. Chem.* **1998**, *37*, 2476.
(17) Wołowiec, S.; Latos-Grażyński, L.; Toronto, D.; Marchon, J.-C. *Inorg. Chem.* **1998**, *37*, 724.
(18) Simonato, J.-P.; Pécaut, J.; Le Pape, L.; Oddou, J.-L.; Jeandey, C.; Shang, M.; Scheidt, W. R.; Wojaczyński, J.; Wołowiec, S.; Latos-Grażyński, L.; Marchon, J.-C. *Inorg. Chem.* **2000**, *39*, 3978.
(19) Latos-Grażyński, L.; Lisowski, J.; Olmstead, M. M.; Balch, A. L. *Inorg. Chem.* **1989**, *28*, 1183.
(20) Balch, A. L.; Cornman, C. R.; Latos-Grażyński, L.; Olmstead, M. M. *J. Am. Chem. Soc.* **1990**, *112*, 7552.
(21) Pawlicki, M.; Latos-Grażyński, L. *Inorg. Chem.* **2002**, *41*, 5866.
(22) Ohgo, Y.; Neya, S.; Ikeue, T.; Takahashi, M.; Takeda, M.; Funasaki, N.; Nakamura, M. *Inorg. Chem.* **2002**, *41*, 4627.
(23) Rachlewicz, K.; Latos-Grażyński, L.; Vogel, E. *Inorg. Chem.* **2000**, *39*, 3247.
(24) Rachlewicz, K.; Latos-Grażyński, L.; Vogel, E.; Ciunik, Z.; Jerzykiewicz, L. *Inorg. Chem.* **2002**, *41*, 1979.
(25) Rachlewicz, K.; Wang, S.-L.; Ko, J.-L.; Hung, C.-H.; Latos-Grażyński, L. *J. Am. Chem. Soc.* **2004**, *126*, 4420.
(26) Kadish, K. M.; Tabard, A.; Van Caemelbecke, E.; Aukauloo, A. M.; Richard, P.; Guilard, R. *Inorg. Chem.* **1998**, *37*, 6168.
(27) Tomizaki, K.; Lysenko, A. B.; Taniguchi, M.; Lindsey, J. S. *Tetrahedron* **2004**, *60*, 2011.
(28) Arnold, D. P.; Johnson, A. W.; Mahendran, M. *J. Chem. Soc., Perkin Trans. 1* **1978**, 366.
(29) Proess, G.; Panker, D.; Hevesi, L. *Tetrahedron Lett.* **1992**, *33*, 269.
(30) Krivokapic, A.; Cowley, A. R.; Anderson, H. L. *J. Org. Chem.* **2003**, *68*, 1089.
(31) Anderson, H. L. *Tetrahedron Lett.* **1992**, *33*, 1101.
(32) Milgrom, L.; Yahioglu, G. *Tetrahedron Lett.* **1995**, *36*, 9061.
(33) Milgrom, L.; Rees, R. D.; Yahioglu, G. *Tetrahedron Lett.* **1997**, *38*, 4905.
(34) Jiang, B.; Yang, S.-W.; Barbini, D. C.; Jones, W. E., Jr. *Chem. Comun.* **1998**, 213.
(35) Plater, M. J.; Aiken, S.; Bourhill, G. *Tetrahedron* **2002**, *58*, 2415.
(36) Anderson, H. L.; Wylie, A. P.; Prout, K. *J. Chem. Soc., Perkin Trans. 1* **1998**, 1607.
(37) LeCours, S. M.; Guan, H.-V.; DiMagno, S. G.; Therien, M. J. *J. Am. Chem. Soc.* **1996**, *118*, 1497.
(38) Arnold, D. P.; Hartnell, R. D. *Tetrahedron* **2001**, *57*, 1335.
(39) Arnold, D. P.; Heath, G. A.; James, D. A. *New J. Chem.* **1998**, *22*, 1377.
(40) Anderson, H. L. *Chem. Commun.* **1999**, 2323.
(41) Shediac, R.; Gray, M. H. B.; Uyeda, H. T.; Johnson, R. C.; Hupp, J. T.; Angiolillo, P. J.; Therien, M. J. *J. Am. Chem. Soc.* **2000**, *122*, 7017.
(42) Burrell, A. K.; Officer, D. L.; Plieger, P. G.; Reid, D. C. W. *Chem. Rev.* **2001**, *101*, 2751.
(43) Gust, D.; Moore, T. A.; Moore, A. L. *Acc. Chem. Res.* **2001**, *34*, 40.
(44) Harvey, P. D. Recent Advances in Free and Metalated Multi-Porphyrin Assemblies and Arrays. A Photophysical Perspective. In *The Porphyrin Handbook*; Kadish, K. M., Smith, K. M., Guilard, R., Eds.; Academic Press: New York, 2003; pp 63−250.

Chart 1

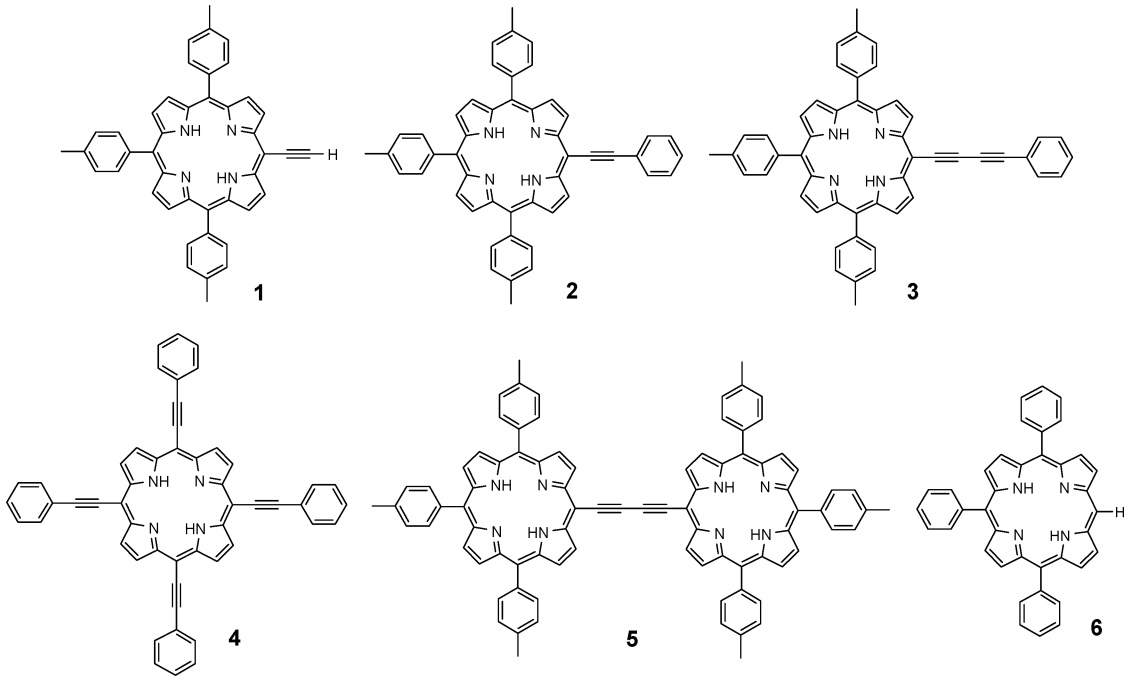

elements have been considered as specifically efficient in the transmission of electronic effects along multipart polyporphyrinic systems.[27,45,46] Appropriately chosen meso substituents, containing ethynyl, phenylethynyl, and phenylbutadiynyl groups, will provide insight into the spin density delocalization in the ethynyl-fragment-containing framework.

Results and Discussion

Synthesis of Ethynylporphyrins and Their Zinc(II) and Iron(III) Complexes. The ethynylporphyrins 5-ethynyl-10,15,20-tri(*p*-tolyl)porphyrin [(ETrTP)H_2, **1**], 5-(phenylethynyl)-10,15,20-tri(*p*-tolyl)porphyrin [(PETrTP)H_2, **2**], 5-(phenylbutadiynyl)-10,15,20-tri(*p*-tolyl)porphyrin [(PBTrTP)H_2, **3**], 5,10,15,20-tetra(phenylethynyl)porphyrin [(TPEP)H_2, **4**], and 1,4-bis-[10,15,20-tri(*p*-tolyl)porphyrin-5-yl]-1,3-butadiyne {[(TrTP)H_2]$_2$B, **5** (B-butadiyne)} were synthesized by procedures previously described in the literature.[31,32,36,47,48]

(TPEP)H_2, **4**, was characterized by X-ray crystallography as a porphyrin dication in the crystal of [(TPEP)H_4](CF_3-$COO)_2$·$(CF_3COOH)_{2.73}$·$(CH_2Cl_2)_{0.27}$. A perspective view of the dication is shown in Figure 1.

The dication **4**-H_2^{2+} presents a significantly saddle-distorted macrocylic conformation. The average deviation of the C_β atoms from the mean plane is 0.574 Å (0.262 Å for all 24 macrocycle atoms). On each porphyrin face, a trifluoroacetate (TFA) anion acts as a monodentate ligand and binds through a carboxyl oxygen to two opposing N−H protons. Each coordinated anion is associated with the

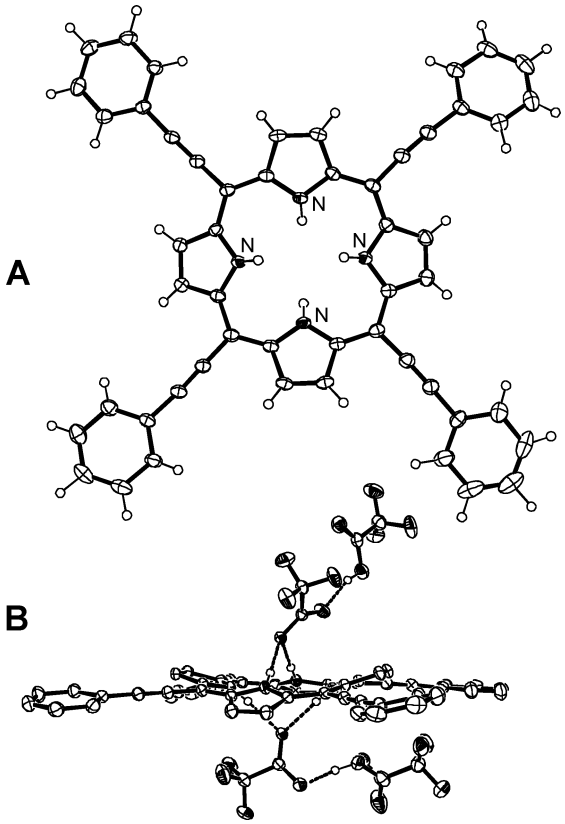

Figure 1. Molecular structure of [(TPEP)H_4]$(CF_3COO)_2$·$(CF_3COOH)_{2.73}$·$(CH_2Cl_2)_{0.27}$ (with 50% probability ellipsoids). In trace A, the TFA anions, TFAH molecules, and CH_2Cl_2 molecule are omitted for clarity. Trace B shows two molecules of TFAH associated with coordinated TFA anions on both faces of the porphyrin plane. The unit cell also contains the site shared by CH_2Cl_2 and TFAH (0.27 and 0.73 occupancy, respectively). Dashed lines indicate hydrogen bonds. The coplanarity of the porphyrin plane and phenylethynyl substituents is visible. The bond lengths in the ethyne unit are C_{meso}−C, 1.419(3)−1.427(3) Å; C≡C, 1.197(3)−1.199(3) Å; and C−C_{ipso}, 1.431(3)−1.437(3) Å.

(45) Piet, J. J.; Taylor, P. N.; Anderson, H. L.; Osuka, A.; Warman, J. M. *J. Am. Chem. Soc.* **2000**, *122*, 1749.
(46) Rubtsov, I. V.; Susumu, K.; Rubtsov, G. I.; Therien, M. J. *J. Am. Chem. Soc.* **2003**, *125*, 2687.
(47) Lin, V. S.-Y.; Therien, M. J. *Chem. Eur. J.* **1995**, *1*, 645.
(48) Koshushkov, S.; Haumann, T.; Boese, R.; Burkhardt, K.; Scheib, S.; Buerle, P.; de Meijere, A. *Angew. Chem., Int. Ed. Engl.* **1995**, *34*, 781.

trifluoroacetic acid (TFAH) molecule via the hydrogen bond. The pyrrole rings are twisted with respect to each other by 23.0(2)°−27.9(2)°. The porphyrin dication **4**-H_2^{2+} presents a degree of porphyrin distortion similar to that seen for the octaethylporphyrin dication $[(OEP)H_4](CF_3COO)_2 \cdot (CF_3COOH)_2$,[49] which is in contrast to *meso*-tetraarylporphyrin dications showing a similar nonplanar saddle conformation but with C_β displacements varying in the 0.9−1.2 Å range.[49−52]

The angles between the planes of the phenyl rings and that of the porphyrin for **4**-H_2^{2+} are 4.6(2)°, 9.6(2)°, 12.4(2)°, and 16.5(2)°. These values are significantly smaller than the corresponding dihedral angles measured for the pyridine zinc complex of 5,10,15,20-tetra(4-butylphenylethynyl)porphyrin where the relevant angles are equal to 29.7(3)° and 59.5(3)° for the two types of aryl rings.[36] However, the nearly coplanar arrangement was previously reported for metalloporphyrins containing one or two aryl moieties linked by ethynyl units at meso positions.[53,54] In *meso*-tetraarylporphyrins, the steric repulsion between the pyrrole hydrogen and the ortho aromatic hydrogens favors torsional angles of around 71°.[55,56] However, the formation of *meso*-tetraarylporphyrin dications results in a large degree of the in-plane rotation of *meso*-aryl groups exemplified by 21° determined for $(TPP)H_4^{2+}$.[50] At present, we assume that the formation of the *meso*-tetraphenylethynylporphyrin dication prefers the nearly coplanar arrangement of the phenyls and the porphyrin plane. These torsional angles can be also determined by crystal packing as a barrier to phenyls rotation, which is expected to be very small compared to that for *meso*-tetraarylporphyrins.

Still, the coplanarity of the porphyrin and phenylethynyl moieties can account for the increased interaction between the porphyrin and phenylethynyl π systems. This phenomenon can explain the enormous bathochromic shifts in the UV−visible electronic spectrum of $(TPEP)H_2$ with respect to those of $(TPP)H_2$ and tetra(trimethylsilylethynyl)porphyrin.[32]

The insertion of iron into ethynylporphyrins resulted in the formation of $(ETrTP)Fe^{III}Cl$ (**1**-FeCl), $(PETrTP)Fe^{III}Cl$ (**2**-FeCl), $(PBTrTP)Fe^{III}Cl$ (**3**-FeCl), $(TPEP)Fe^{III}Cl$ (**4**-FeCl), and $[(TrTP)Fe^{III}Cl]_2B$ [**5**-$(FeCl)_2$]. The electronic spectra of high-spin iron(III) ethynylporphyrins (Figure 2) are characteristic for high-spin iron(III) tetraphenylporphyrins.[57] The extension of the aromatic system causes bathochromic shifts

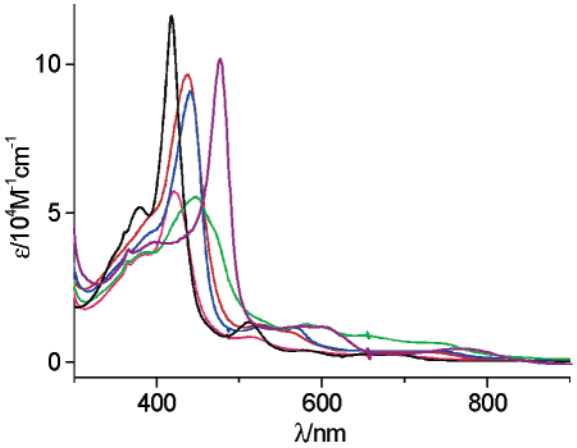

Figure 2. Electronic spectra of **1**-FeCl (pink), **2**-FeCl (red), **3**-FeCl (blue), **4**-FeCl (purple, spectrum for the saturated solution), **5**-FeCl (green), and $(TPP)Fe^{III}Cl$ (black) in chloroform.

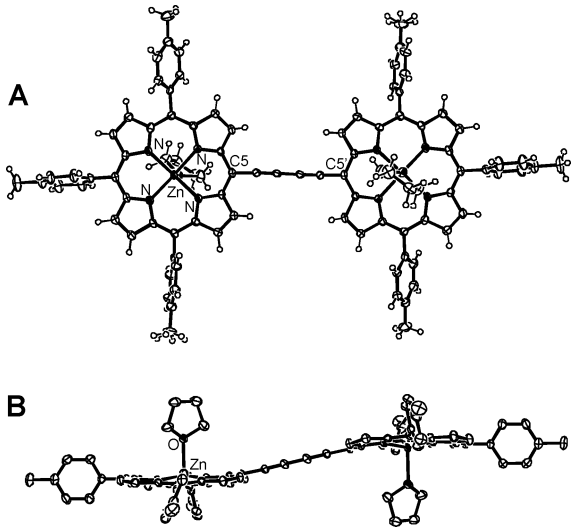

Figure 3. Molecular structure of bis-tetrahydrofuran 1,4-bis-[10,15,20-tri(*p*-tolyl)porphyrinatozinc(II)-5-yl]-1,3-butadiyne (**5**-Zn_2) (with 50% probability ellipsoids). Trace B emphasizes the mutual arrangement of two subunits. The bond lengths in the central butadiyne unit are C_{meso}−C, 1.422(3) Å; C≡C, 1.204(4) Å; and central C−C, 1.373(6) Å.

of all bands and changes in their relative intensity as compared to those in the spectrum of $(TPP)Fe^{III}Cl$.

Zinc(II) is readily inserted into **1**−**5** by a standard metalation procedure to yield (ETrTP)Zn (**1**-Zn), (PETrTP)Zn (**2**-Zn), (PBTrTP)Zn (**3**-Zn), (TPEP)Zn (**4**-Zn), and $[(TrTP)Zn]_2B$ (**5**-Zn_2). The synthesis of zinc(II) complexes was prompted by the fact that these complexes have been applied as suitable diamagnetic standards in the analysis of ^{1}H NMR spectra of the corresponding iron(III) ethynylporphyrins. The ^{1}H NMR parameters of zinc(II) ethynylporphyrins are given in the Supporting Information.

The bis-tetrahydrofuran 1,4-bis-[10,15,20-tri(*p*-tolyl)porphyrinatozinc(II)-5-yl]-1,3-butadiyne (**5**-Zn_2) complex was characterized by X-ray crystallography (Figure 3). The complex contains two $[(TrTP)Zn^{II}(THF)]$ subunits resembling the zinc(II) 5,10,15-tri(*p*-metoxyphenyl)porphyrin {[Tr(*p*-MeOP)P]Zn^{II}}.[58] Actually, the bond lengths and angles of

(49) Senge, M. O.; Forsyth, T. P.; Nguyen, L. T.; Smith, K. M. *Angew. Chem., Int. Ed. Engl.* **1994**, *33*, 2485.
(50) Stone, A.; Fleischer, E. B. *J. Am. Chem. Soc.* **1968**, *90*, 2736.
(51) Senge, M. O.; Kalisch, W. W. *Z. Naturforsch. B: Chem. Sci.* **1999**, *54*, 943.
(52) Cetinkaya, E.; Johnson, A. W.; Lappert, M. F.; McLaughlin, G. M.; Muir, K. W. *J. Chem. Soc., Dalton Trans.* **1974**, 1236.
(53) LeCours, S. M.; DiMagno, S. G.; Therien, M. J. *J. Am. Chem. Soc.* **1996**, *118*, 11854.
(54) Yeung, M.; Ng, A. C. H.; Drew, M. G. B.; Vorpagel, E.; Breitung, E. M.; McMahon, R. J.; Ng, D. K. P. *J. Org. Chem.* **1998**, *63*, 7143.
(55) Silver, A.; Tulinsky, A. *J. Am. Chem. Soc.* **1964**, *86*, 927.
(56) Huuskonen, S. P. J.; Wilson, G. S.; Anderson, H. L. *Acta Crystallogr. C: Cryst. Struct. Commun.* **1998**, *54*, 662.
(57) Wojaczyński, J.; Latos-Grażyński, L.; Głowiak, T. *Inorg. Chem.* **1997**, *36*, 6299.
(58) Wojaczyński, J.; Latos-Grażyński, L.; Chmielewski, P. J.; Van Calcar, P.; Balch, A. L. *Inorg. Chem.* **1999**, *38*, 3040.

Chart 2

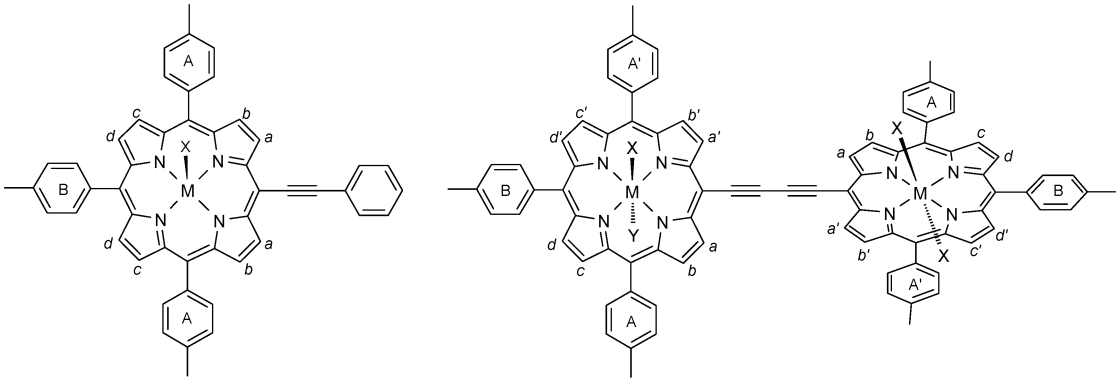

the two subunits are within the limits expected for zinc(II) porphyrins.[58] The porphyrin macrocycle of [(TrTP)Zn^{II}(THF)] adopts a ruffled conformation. The zinc, which axially coordinates a THF molecule, is displaced from the average porphyrin plane by 0.324(1) Å. The butadiyne linker is practically linear. Actually, the C(5) and C(5′) *meso*-carbons are nearly located on the straight line defined by butadiyne carbon atoms. The porphyrin planes of the subunits are parallel in the solid state resulting from a crystallographic inversion center located in the center of the molecule. However, free rotation around the butadiyne unit is expected in solution.[36]

The distance between the two planes defined by the four nitrogen atoms of each porphyrinic subunit equals 1.72(2) Å. Previously, Anderson and co-workers structurally characterized the pyridine zinc(II) *meso*-butadiyne linked dimer derived from 5,15-bis(3,5-di-*tert*-butylphenyl)-10,20-bis(trihexylsilylethynyl)porphyrin.[59] This dimer containing a 56-atom π system is remarkably planar (to ±0.391 Å). The displacement range from the 52-atom plane of **5**-Zn_2 is markedly larger (to ±0.587 Å). In the two dimers, the bond lengths of the butadiyne unit are comparable.

High-Spin Iron(III) Porphyrin ^{1}H NMR Studies. To understand the spectral data, the structural characteristics of metalloporphyrins were considered. The monomeric complexes containing the tri(*p*-tolyl)porphyrin unit (ethynylporphyrins **1**, **2**, **3**) will have the highest maximal C_{2v} symmetry when the corresponding metalloporphyrin has identical ligation on both sides of the porphyrin plane or C_s symmetry when the ligation on either side is different. In both cases, four distinct types of pyrrole protons (labeled a−d for **2**-MX in Chart 2) and two types of phenyl groups (labeled A and B) are present. C_{4v} symmetry is expected in the case of complexes derived from **4** yielding a single β-H resonance.

For the dimeric porphyrin **5**-M_2 (X,Y positions not occupied) with simple planar coordination in each macrocycle, the molecule exhibits at least the D_2 symmetry. In Chart 2, this dimer is shown with two subunits in different planes, as fast rotation around butydiyne linker is expected. In the **5**-M_2 dimer, again four distinct types of pyrrole protons labeled a−d and two types of *p*-tolyl groups (labeled A and B) are present (the primed positions, a′−d′ and A′, are symmetry equivalent to the a−d and A sets). The analysis carried out for four-coordinate [(TrTP)M]$_2$B (**5**-M_2) holds for the six-coordinate [(TrTP)Fe(CN)$_2$]$_2$B {**5**-[Fe(CN)$_2$]$_2$} as well. For the dimeric [(TrTP)Fe^{III}Cl]$_2$B [**5**-(FeCl)$_2$], the spectroscopic pattern can be more complicated. The ionic radius and charge of the high-spin iron(III) impose five-coordinate square-pyramidal structures on each [(TrTP)Fe^{III}Cl] subunit. Accordingly, these metal ions are displaced from the porphyrin plane. The two subunits of [(TrTP)Fe^{III}Cl]$_2$B [**5**-(FeCl)$_2$] are not necessarily coplanar. The dimeric molecule has C_2 symmetry with the C_2 axis perpendicular to the C(5)−C(5′) linker. Thus two [(TrTP)Fe^{III}Cl] subunits are equivalent. However, as seen in Chart 2, the pyrrolic positions 7-H(a) and 3-H(a′), 8-H(b) and 2-H(b′), 12-H(c) and 18-H(c′), and 13-H(d) and 17-H(d′) are no longer equivalent, in contrast to [(TrTP)M]$_2$B (**5**-M_2). Additionally, the symmetry lowering in these five-coordinate complexes renders the three tolyls substituents on each porphyrin inequivalent. Such a geometry has been reflected in the ^{1}H NMR spectrum of the previously investigated iron(III) 5,5′-bis(10,15,20-triphenylporphyrin) {[(TrPP)Fe^{III}Cl]$_2$} with direct meso−meso linkage of two iron(III) porphyrinic subunits.[58] In contrast to [(TrPP)Fe^{III}Cl]$_2$, where the steric hindrance of the adjacent pyrrolic fragments hinders rotation around the meso−meso linkage, fast rotation around the butadiyne linker is sterically allowed for [(TrTP)Fe^{III}Cl]$_2$B [**5**-(FeCl)$_2$]. Thus, the number of β-H pyrrole resonances will be reduced to four. Consequently, only two sets of *meso*-(*p*-tolyl) resonances are predicted. On each *meso*-tolyl ring, the two ortho and two meta protons are not equivalent because the porphyrin plane bears different substituents on opposite sides and rotation about the *meso*-carbon−tolyl bond is restricted. On the other hand, two ortho, two meta, and two *p*-methyl resonances are expected when two porphyrin sides are identical {e.g., the six-coordinate complex [(TrTP)-Fe(CN)$_2$]$_2$B, **5**-[Fe(CN)$_2$]$_2$}.

Respective ^{1}H NMR spectra for high-spin iron(III) ethynylporphyrins are presented in Figures 4 and 5. For the sake of comparison, the spectrum of chloroiron(III) 5,10,15-triphenylporphyrin (TrPP)Fe^{III}Cl (**6**-FeCl) has been included in Figure 4 (trace A). The spectral parameters are gathered in Table 1. Resonance assignments, which are given above selected peaks, were made on the basis of relative intensities and line widths. The plots of temperature dependence of the

(59) Taylor, P. N.; Huuskonen, J.; Rumbles, G.; Aplin, R. T.; Williams, E.; Anderson, H. L. *Chem. Commun.* **1998**, 909.

Table 1. Chemical Shifts of High-Spin Iron(III) Ethynylporphyrins

		phenyl			tolyl		
compound	pyrrole	ortho	meta	para	ortho	meta	methyl
(ETrTP)$Fe^{III}Cl$ (**1**-FeCl)[a,b]	78.4, 79.4	–	–	–	5.4, 8.1	11.4, 11.8, 12.5, 13.0	5.9, 6.2
(PETrTP)$Fe^{III}Cl$ (**2**-FeCl)[a]	77.8, 78.6, 80.1	2.2	11.5	0.8	5.3, 8.3	11.5, 11.9, 12.7, 13.0	6.1, 6.3
(PBTrTP)$Fe^{III}Cl$ (**3**-FeCl)[a]	78.0, 79.5	4.8	9.5	4.3	8.4	11.2, 11.6, 12.3, 12.8	5.8, 6.1
(TPEP)$Fe^{III}Cl$ (**4**-FeCl)[a]	75.7	4.1	10.7	2.7	–	–	–
[(TrTP)$Fe^{III}Cl]_2B$ (**5**-FeCl)[a]	77.8, 78.5, 79.1	–	–	–	8.7	11.2, 11.7, 12.4, 12.8	5.8, 6.2
(TrPP)$Fe^{III}Cl$ (**6**-FeCl)[c]	78.5, 81.1, 81.9	5.1, 8.2	12.1, 12.3, 13.3, 13.5	6.4, 6.5	–	–	–

[a] Measured in chloroform-*d* at 298 K. [b] Ethynyl-H, −45.4 ppm. [c] Measured in chloroform-*d* at 293 K; *meso*-H, −72.4 ppm.[59]

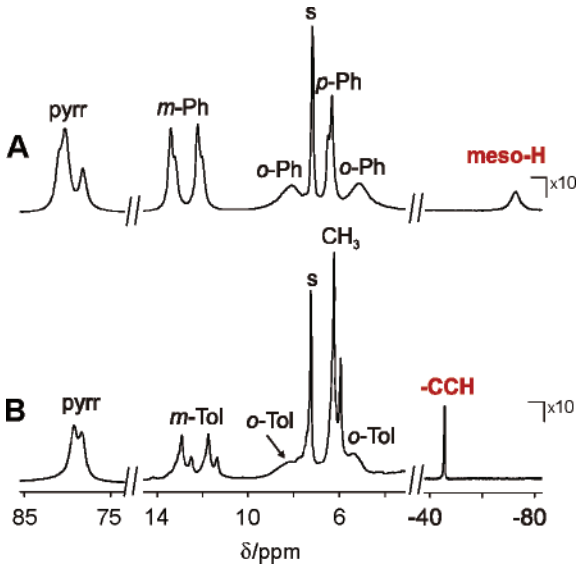

Figure 4. ^{1}H NMR spectra of (A) (TrPP)$Fe^{III}Cl$ (**6**-FeCl) and (B) (ETrTP)-$Fe^{III}Cl$ (**1**-FeCl) in chloroform-*d* at 298 K. Resonance assignments: *o*-Ph, *m*-Ph, and *p*-Ph, *ortho*-, *meta*-, and *para*-phenyl protons, respectively; *o*-Tol and *m*-Tol, *ortho*- and *meta*-tolyl protons, respectively; pyrr, pyrrole protons; CH_3, methyl protons of the tolyl; *meso*, *meso*-proton; −CCH, ethynyl proton; s, solvent. The relative intensity of the 70−90 ppm region has been increased by a factor of 3.

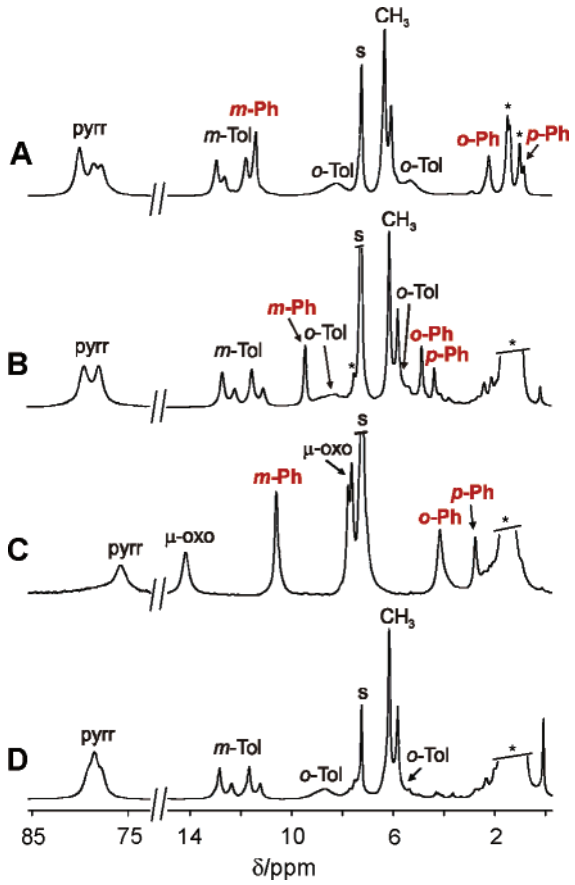

Figure 5. ^{1}H NMR spectra of (A) (PETrTP)$Fe^{III}Cl$ (**2**-FeCl), (B) (PBTrTP)$Fe^{III}Cl$ (**3**-FeCl), (C) (TPEP)$Fe^{III}Cl$ (**4**-FeCl, generated by titration of the μ-oxo dimer **4**-Fe_2O by chloroform-*d* saturated with HCl), and (D) [(TrTP)$Fe^{III}Cl]_2B$ [**5**-$(FeCl)_2$] in chloroform-*d* at 298 K. Resonance assignments: μ-oxo, protons of μ-oxo dimer **4**-Fe_2O; *, impurities; all others follow those of Figure 4. The relative intensity of the 70−90 ppm region in all traces has been increased by a factor of 3.

chemical shifts, which are typical for the high-spin iron(III) electronic state of iron porphyrins, are shown in the Supporting Information. Direct comparisons to iron(III) tetraphenylporphyrin derivatives facilitated the assignment.[1,8,57,58,60]

Thus, the eight equivalent β-pyrrole positions of (TPEP)-$Fe^{III}Cl$ (**4**-FeCl) produce a singlet at 75.7 ppm. The four unequivalent pyrrole positions of **1**-FeCl, **2**-FeCl, and **3**-FeCl are expected to generate four downfield-shifted pyrrole resonances for well-resolved spectra. Severe overlapping of relatively broad resonances reduces this number to three or two, accompanied by the appropriate alteration of intensities. The characteristic meso-substituent dependent patterns, are demonstrated in Figures 4 and 5. These pyrrolic resonances are spread near the position typical for high-spin iron(III) tetraphenylporphyrins, i.e., ca. 80 ppm (298 K), resembling spectra of others meso-substituted high-spin iron(III) 5-X-triarylporphyrin complexes (X = H, NO_2, Br, OAc, OH).[8,58] The *meso*-(*p*-tolyl) resonances are located in the region that is typical for high-spin iron(III) porphyrins. The multiplicity of the respective resonances is directly related to the symmetry of molecules as discussed in detail above. Thus, for **1**-FeCl, **2**-FeCl, and **3**-FeCl, the characteristic well-resolved pattern of *meta*-(*p*-tolyl) resonances was detected. In each case, the pattern consists of two doublets with a 2:1 intensity ratio, readily assigned to A and B meso positions. The presence of two lines for one meso substituent confirms the slow *p*-tolyl rotation around the $C_{meso}-C_{ipso}$ bond. The ^{1}H NMR spectrum of dimeric [(TrTP)$Fe^{III}Cl]_2B$ [**5**-$(FeCl)_2$] matches the spectra of the above-described monomeric species as far as the pyrrolic and *meta*-(*p*-tolyl) resonances are concerned. This observation is consistent with the anticipated free rotation around the butadiyne unit.

Considering the fact that the iron(III) tri(*p*-tolyl)porphyrin fragment is common for all compounds under investigation, the identification of other paramagnetic shifted resonances is straightforward by default. This spectroscopic task is of

(60) Wojaczyński, J.; Latos-Grażyński, L. *Inorg. Chem.* **1995**, *34*, 1044.

primary importance, as the delocalization of the spin density along the ethynyl or butadiynyl fragment is the main interest of the presented project. The respective assignments are given in Figures 4 and 5 and in Table 1. As seen in Figure 4 (trace B), this is the single resonance in the far upfield region that can be assigned to the ethynyl proton of **1**-FeCl. The position resembles that of the *meso*-H resonance of **6**-FeCl (Figure 4, trace A). Significantly, the difference in line widths is remarkable despite the identical axial ligation. In contrast, the other resonances (β-H and *meta*-H of *meso*-aryls) of **1**-FeCl and **6**-FeCl reveal similar line widths. Paramagnetically induced broadening can be of both dipolar and scalar origin, but the scalar contribution is typically small. The dipolar contribution to the line width broadening is presumed to be proportional to r^{-6}, where r is the distance from the paramagnetic center to the proton in question.[61,62] Thus, the marked difference in line widths seen for *meso*-H of **6**-FeCl and ethynyl-H of **1**-FeCl clearly reflects the distance from the paramagnetic center and is consistent with the proposed assignment. Analogously, relatively narrow resonances were detected for the phenyls capping ethynyl or butadiynyl moieties of **2**-FeCl, **3**-FeCl, and **4**-FeCl as compared to (TPP)Fe^{III}Cl where *meso*-phenyls are directly linked to the *meso*-carbon.

***μ*-Oxo-Bridged Diiron Complexes.** Treatment of the high-spin iron(III) ethynylporphyrins **1**-FeCl, **2**-FeCl, **3**-FeCl, and **4**-FeCl with K_2CO_3 in water or chromatography on a basic alumina column resulted in formation of the μ-oxo-bridged diiron complexes [(ETrTP)Fe^{III}]$_2$O (**1**-Fe_2O), [(PETrTP)-Fe^{III}]$_2$O (**2**-Fe_2O), [(PBTrTP)Fe^{III}]$_2$O (**3**-Fe_2O), and [(TPEP)-Fe^{III}]$_2$O (**4**-Fe_2O). The ^{1}H NMR patterns of **1**-Fe_2O, **2**-Fe_2O, and **3**-Fe_2O, which spread in the 12−16 ppm range, are reproduced by a convolution of four pyrrole resonances and reflect the symmetry of the iron(III) tri(*p*-tolyl)porphyrin subunit. As expected, a single pyrrole line was detected for symmetrical **4**-Fe_2O. These β-H resonances demonstrate the anti-Curie behavior of the isotropic shifts, i.e., an increase of the pyrrole resonance shifts on warming, as expected for μ-oxo-bridged diiron porphyrins.[63] The spectral properties resemble those of asymmetric tetraphenylporphyrin derivatives including μ-oxo-bridged diiron complexes of *N*-methylporphyrin, 21-oxaporphyrin, and recently characterized μ-oxo diiron(III) 5,10,15-triphenylporphyrin (**6**-Fe_2O) [δ, 13.2 (4H), 13.4 (4H), 13.6 (8H), *meso-H* (2H) 6.3 ppm, 293 K].[21,58,64] The ethynyl-H resonance of **1**-Fe_2O is expected in the region of intense solvent signals (1−2 ppm).

The ^{1}H NMR studies indicate that chromatography of [(TrTP)Fe^{III}Cl]$_2$B [**5**-$(FeCl)_2$] on a basic alumina column yields a single product with the ^{1}H NMR spectroscopic features of the μ-oxo-bridged diiron(III) fragment −(TrTP)-$Fe_{III}OFe^{III}$(TrTP)− characterized above in detail for **1**-Fe_2O, **2**-Fe_2O, **3**-Fe_2O, and **6**-Fe_2O. Specifically, the well-resolved set of four pyrrole resonances at 13.0, 13.3, 13.7, and 15.0 ppm (298 K) that reflects anti-Curie behavior was identified (Figure 6).

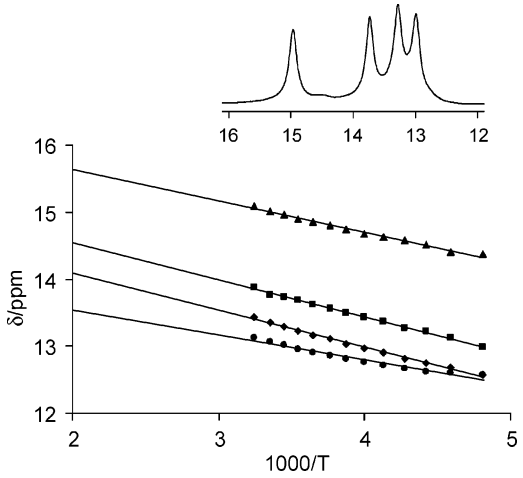

Figure 6. Plot of chemical shifts versus $1/T$ for the cyclic [(TrTP)Fe^{III}-OFe^{III}(TrTP)-B]$_2$ [**5**$_2$-$(FeOFe)_2$] complex with two μ-oxo bridges linking subunits of two iron diporphyrins connected by the butadiyne linker. The solid lines are for illustrative purposes only. Inset: Pyrrolic fragment of the ^{1}H NMR spectrum (298 K, $CDCl_3$).

The feasible formation of the high-spin (TrTP)Fe^{III}OH moiety has not been documented in the conditions of our experiments. The possible hydroxy species were expected to be discerned by a set of resonances resembling those of the precursor [(TrTP)Fe^{III}Cl]$_2$B [**5**-$(FeCl)_2$]. The analytically significant pyrrole resonances of [(TrTP)Fe^{III}(OH)]$_2$B [**5**-$(FeOH)_2$] or [(TrTP)Fe^{III}Cl]B[(TrTP)Fe^{III}OH] [**5**-(FeCl)-(FeOH)] would be broader than the resonances of **5**-$(FeCl)_2$, as is characteristic for the hydroxy group coordination to iron(III) porphyrins.[65,66] Scheme 1 presents one feasible route resulting in the formation of a variety species containing μ-oxo diiron units. The gradual replacement of chloride by hydroxide initially produces [(TrTP)Fe^{III}Cl]B[(TrTP)Fe^{III}OH] [**5**-(FeCl)(FeOH)], followed by [(TrTP)Fe^{III}(OH)]$_2$B [**5**-$(FeOH)_2$]. Subsequent condensation (dehydratation) generates the μ-oxo-bridged diiron(III) fragment −(TrTP)$Fe^{III}OFe^{III}$-(TrTP)−, which can be built into the more elaborate molecular structures as shown in Scheme 1. For instance, in (HOFe)-**5**-(FeOFe)-**5**-(FeOH), the terminal subunits remain high-spin five-coordinate with the OH group in the axial position, which has been excluded on the basis of the ^{1}H NMR evidence. The flexibility of [(TrTP)Fe^{III}Cl]$_2$B [**5**-$(FeCl)_2$] allows for the formation of the cyclic [(TrTP)$Fe_{III}OFe^{III}$-(TrTP)-B]$_2$ [**5**-$(FeOFe)_2$] complex with two μ-oxo bridges linking subunits of two diiron diporphyrins connected by the butadiyne linker. The structure of **5**-$(FeOFe)_2$ was unambiguously confirmed by mass spectrometry (m/z = 2662.0; calcd for $C_{172}H_{116}N_{16}O_2Fe_4$ 2662.3).

Previoulsy, Anderson and co-workers demonstrated that the zinc(II) complexes of the conjugated porphyrin oligomers,

(61) La Mar, G. N.; Walker, F. A. NMR of Paramagnetic Porphyrins. In *The Porphyrins*; Dolphin, D., Ed.; Academic Press: New York, 1979; pp 57−161.
(62) Bertini, I.; Luchinat, C. *Coord. Chem. Rev.* **1996**, *150*, 1.
(63) Boersma, A. D.; Phillippi, M. A.; Goff, H. M. *J. Magn. Reson.* **1984**, *57*, 197.
(64) Wysłouch, A.; Latos-Grażyński, L.; Grzeszczuk, M.; Drabent, K.; Bartczak, T. *J. Chem. Soc., Chem. Commun.* **1988**, 1377.
(65) Cheng, R.-J.; Latos-Grażyński, L.; Balch, A. L. *Inorg. Chem.* **1982**, *21*, 2412.
(66) Balch, A. L.; Chan, Y.-W.; Cheng, R.-J.; La Mar, G. N.; Latos-Grażyński, L.; Renner, M. W. *J. Am. Chem. Soc.* **1984**, *106*, 7779.

Scheme 1

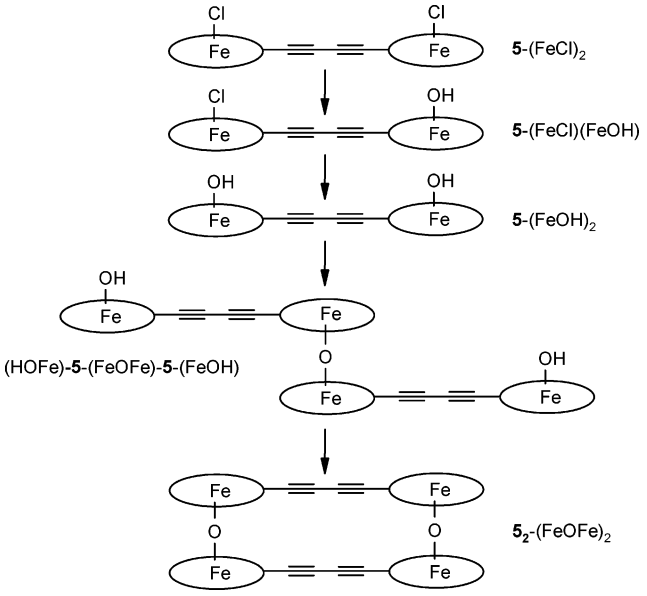

from the dimer to the hexamer, form stable ladder complexes with 1,4-diazabicyclo[2.2.2]octane and 4,4′-bipyridyl.[67,68] The geometry of **5**-(FeOFe)$_2$ resembles that of the 2:2 ladder dimer with the 1,4-diazabicyclo[2.2.2] coordinating linker.[68]

Spectral Characterization of Low-Spin Iron(III) Ethynylporphyrins. Titration of **1**-FeCl, **2**-FeCl, **3**-FeCl, **4**-FeCl, and **5**-(FeCl)$_2$ dissolved in chloroform-*d* with an excess of potassium cyanide in methanol-d_4 results in their conversion to the six-coordinate low-spin complexes [(ETrTP)Fe^{III}(CN)$_2$] [**1**-Fe(CN)$_2$], [(PETrTP)Fe^{III}(CN)$_2$] [**2**-Fe(CN)$_2$], [(PBTrTP)-Fe^{III}(CN)$_2$] [**3**-Fe(CN)$_2$], [(TPEP)Fe^{III}(CN)$_2$] [**4**-Fe(CN)$_2$], and {[(TrTP)Fe^{III}(CN)$_2$]$_2$B}^{2} {**5**-[Fe(CN)$_2$]$_2$}, respectively. Nearly identical spectra were generated by dissolution of the respective iron(III) ethynylporphyrin in methanol-d_4 saturated with potassium cyanide. The assignment of the ethynyl-H resonance of **1**-Fe(CN)$_2$ was possible only in the first stage of titration of **1**-FeCl in chloroform-*d* with KCN in methanol-d_4. In this experiment, selective deuteration at this particular position took place with methanol-d_4 as the source of deuterium. The deuteration was confirmed by an independent experiment. Specifically, after titration in the presence of methanol-d_4, when the deuteration had been completed, the sample was dried and redissolved in chloroform-*d* in the presence of (TBA)CN (tetrabutylammonium cyanide). This sample yielded a spectrum resembling that obtained directly by titration of **1**-FeCl with (TBA)CN but with the single ethynyl resonance missing.

Titration of iron(III) ethynylporphyrins with (TBA)CN in chloroform-*d* produced the low-spin bis-cyanide species, although with β-resonances shifted upfield in comparison with the spectra collected in the presence of methanol-d_4. It has already been demonstrated that hydrogen bonding to the cyanide ligand causes a general decrease of [(TPP)Fe^{III}(CN)$_2$] isotropic shifts.[69,70] Thus, the sensitivity of the isotropic shifts

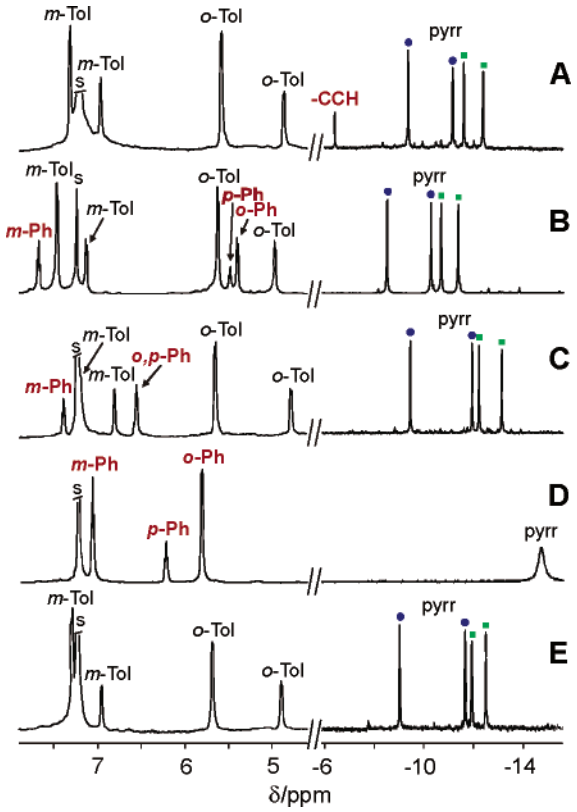

Figure 7. ^{1}H NMR spectra of (A) [(ETrTP)Fe^{III}(CN)$_2$]$^-$ [**1**-Fe(CN)$_2$], (B) [(PETrTP)Fe^{III}(CN)$_2$]$^-$ [**2**-Fe(CN)$_2$], (C) [(PBTrTP)Fe^{III}(CN)$_2$]$^-$ [**3**-Fe(CN)$_2$], (D) [(TPEP)Fe^{III}(CN)$_2$]$^-$ [**4**-Fe(CN)$_2$], and (E) {[(TrTP)Fe^{III}-(CN)$_2$]$_2$B}$^{2-}$ {**5**-[Fe(CN)$_2$]$_2$} in chloroform-*d*/methanol-d_4 solution at 298 K. Resonance assignments follow those of Figures 4 and 5; squares and circles denote the scalar coupled pairs of pyrrole protons. The relative intensity of the region between −6 and −16 ppm in all traces has been increased by a factor of 2.

of bis-cyanide iron(III) ethynylporphyrins to the presence of methanol follows the general trend. Usually, low-spin iron-(III) porphyrins, formed by the coordination of two cyanide ligands, produce very narrow paramagnetically shifted resonances because of their optimal relaxation properties.[5] An excess of potassium cyanide added to **4**-FeCl led to side reactions, as cyanide acts generally as a reducing agent toward iron(III) porphyrins.[7,71] The one-electron reduction introduces [(TPEP)Fe^{II}(CN)$_2$], which remains in fast exchange with the maternal [(TPEP)Fe^{III}(CN)$_2$]. The fast electron exchange causes significant broadening of the pyrrole resonances and their slight shift toward the downfield direction.

Previously, complex equilibria were detected in the course of titration of covalently linked diiron diporphyrins (porphyrin subunits connected by diether aliphatic moieties) with cyanide.[72] Analogously, the stepwise addition of cyanide to a chloroform solution of **5**-(FeCl)$_2$ revealed a multiplicity of species. Here, the final titration product, {[(TrTP)Fe^{III}-(CN)$_2$]$_2$B}$^{2-}$ {**5**-[Fe(CN)$_2$]$_2$}, is the only species analyzed. The representative ^{1}H NMR spectra of **1**-Fe(CN)$_2$, **2**-Fe(CN)$_2$, **3**-Fe(CN)$_2$, **4**-Fe(CN)$_2$, and **5**-[Fe(CN)$_2$]$_2$ are shown in Figure

(67) Anderson, H. L. *Inorg. Chem.* **1994**, *33*, 972.
(68) Taylor, P. N.; Anderson, H. L. *J. Am. Chem. Soc.* **1999**, *121*, 11538.
(69) La Mar, G. N.; Del Gaudio, J.; Frye, J. S. *Biochim. Biophys. Acta* **1977**, *498*, 422.
(70) Ikezaki, A.; Nakamura, M. *Inorg. Chem.* **2002**, *41*, 2761.
(71) La Mar, G. N.; Del Gaudio, J. *Adv. Chem. Ser.* **1977**, *162*, 207.
(72) Wołowiec, S.; Latos-Grażyński, L. *Inorg. Chem.* **1994**, *33*, 3576.

Table 2. Chemical Shifts of Low-Spin Iron(III) Ethynylporphyrins

compound	pyrrole	phenyl			tolyl		
		ortho	meta	para	ortho	meta	methyl
$[(ETrTP)Fe^{III}(CN)_2]^-$ [**1**-$Fe(CN)_2$][a,b]	−9.3, −11.1, −11.5, −12.3	−	−	−	4.9, 5.6	7.0, 7.3	2.5, 2,7
$[(PETrTP)Fe^{III}(CN)_2]^-$ [**2**-$Fe(CN)_2$][a]	−8.5, −10.3, −10.7, −11.4	5.4	7.7	5.5	5.0, 5.6	7.1, 7.5	2.6, 2.8
$[(PBTrTP)Fe^{III}(CN)_2]^-$ [**3**-$Fe(CN)_2$][a]	−9.4, −11.9, −12.2, −13.1	6.5	7.4	6.6	4.8, 5.6	6.8, 7.2	2.3, 2.5
$[(TPEP)Fe^{III}(CN)_2]^-$ [**4**-$Fe(CN)_2$][a]	−14.7	5.8	7.1	6.2	−	−	−
$\{[(TrTP)Fe^{III}(CN)_2]_2B\}^{2-}$ [**5**-$[Fe(CN)_2]_2$][a]	−9.0, −11.7, −11.9, −12.5	−	−	−	4.9, 5.7	7.0, 7.3	2.5, 2.6
$[(TrTP)Fe^{III}(CN)_2]^-$ [**6**-$Fe(CN)_2$][c]	−9.5, −9.7, −10.5, −12.3	5.1, 6.1	7.3, 7.8	6.4, 6.7	−	−	−

[a] Obtained by titration of high-spin iron(III) complexes in chloroform-*d* with KCN in methanol-d_4 at 298 K. [b] Ethynyl-H, −6.3 ppm. [c] Measured in methanol-d_4 at 293 K; *meso*-H, −6.9 ppm.[59]

7. The chemical shift values are collected in Table 2. The characteristic sets of four pyrrole resonances of **1**-$Fe(CN)_2$, **2**-$Fe(CN)_2$, **3**-$Fe(CN)_2$, and **5**-$[Fe(CN)_2]_2$, located in the range between −8 and −13 ppm (298 K), are of importance in describing the ground state of the electronic structure. These pyrrole resonances are accompanied by two sets of ortho and *p*-methyl resonances assigned to *meso*-(*p*-tolyls) that reveal upfield isotropic shifts and corresponding sets of meta resonances with opposite, i.e., downfield, isotropic shifts. In our case, the primary assignment could be made on the basis of the resonance positions, their intensities, and their multiplet structure due to scalar coupling. A two-dimensional COSY experiment was effective in connecting the pyrrole proton resonances in low-spin iron(III) complexes of ethynylporphyrins. We could easily separate the *p*-tolyl proton signals into two subsets, each assigned to individual *meso*-(*p*-tolyls). Significantly, the characteristic coupling of three phenyl resonances in **2**-$Fe(CN)_2$, **3**-$Fe(CN)_2$, and **4**-$Fe(CN)_2$ allowed their direct identification.

Titration with the 1-methylimidazole ligand produced spectra that demonstrate the typical shifts of low-spin iron(III) porphyrins with the $(d_{xy})^2(d_{xz}d_{yz})^3$ ground electronic state.[1]

Spin Density Transfer Along Ethyne or Butadiyne Linkers. The electronic structure of *meso*-ethynyl(s) allows extensive conjugation with the porphyrinic macrocycle readily accounting for the general features of ethynylporphyrins. Geometry optimizations and electronic structure calculations using density functional theory (DFT) have been reported for porphyrins with *meso*-ethynyl substituents.[73] The calculated electronic structures clearly show that the ethynyl group contributes to the π-electron conjugation along the porphyrin ring for the HOMO and LUMO and significantly reduces the HOMO−LUMO gap, consistent with experimental results.[73] The ZINDO calculation carried out for copper(II) 5,15-bis(arylethynyl)-10,20-diphenylporphyrins demonstrated that the frontier molecular orbitals extend on the arylethynyl moiety.[72]

In this context, the introduction of the ethynyl group raises the problem of the impact of such a modification on the electronic properties of the resulting iron(III) porphyrins to be followed by ^{1}H NMR spectroscopy. Evidently, the investigated compounds complete the previously investigated iron(III) 5-X-triarylporphyrin series (X = H, Br, OCH_3, OH, NO_2, $[(TrPP)Fe^{III}]$) characterized in order to elucidate the relationship between the electron-donating/-withdrawing properties of the 5-substituents and the ^{1}H NMR spectral pattern.[58] Actually, the analogous effects of the meso substituent on the geometric and electronic structures of high-spin and low-spin iron(III) meso-substituted octaethylporphyrins $\{[(5\text{-X-OEP})Fe^{III}]$, X = Ph, *n*-butyl, Cl, CN, HCO, $NO_2\}$ were explored as well.[74] To trace the extent of communication via the ethyne or butydiyne fragment, the isotropic shifts of the resonances of the capping fragments, i.e., −H or phenyl, were analyzed in detail in the series −H, −Ph, −CC−H, −CC−Ph, −CC−CC−Ph, −(CC−CC−TrTP)Fe^{III}. Finally, the communication between two iron(III) porphyrinic fragments linked via the butadiyne moiety of **5**-Fe_2 was explored.

First, we used ^{1}H NMR spectroscopy to analyze the influence of meso substitution on the $(TrTP)Fe^{III}$ moiety. A comparison of the isotropic shifts leads to the general conclusion that the β-H patterns are quite similar for each considered set of pairs: $(TrPP)Fe^{III}Cl$ and (5-X-TrTP)Fe^{III}-Cl, $[(TrPP)Fe^{III}(CN)_2]$ and $[(5\text{-X-TrTP})Fe^{III}(CN)]_2$, $[(TrPP)Fe^{III}(1\text{-MeIm})_2]^+$ and $[(5\text{-X-TrTP})Fe^{III}(1\text{-MeIm})]_2^+$ (X = ethynyl, phenylethynyl, phenylbutadiynyl). Thus, monoethynyl substitution barely affects the ground electronic state of the $(TrTP)Fe^{III}$ moiety.

In light of the current interest in applications of porphyrinic arrays,[75] the ethynyl fragment plays a crucial structural role, allowing multiporphyrin covalently linked structures, which act efficiently in energy transfer or as elements in molecular photonic devices,[27] to be built. Apart from their architectural function, the linkers containing ethynyl make available a channel for electronic communication between the porphyrins. The electronic coupling between the porphyrin core and its substituents is optimized by the cylindrical symmetric ethynyl linker. As steric factors do not preclude it, a coplanar arrangement of the involved aromatic ring systems along the molecular axis of the highest conjugation is expected. For instance, a highly extended system is effectively created in 5-phenylethynyl-10,15,20-tri(*p*-tolyl)porphyrin (**2**), leading to the expectation that the phenylethynyl unit and the porphyrin macrocycle will communicate electronically.[27,75,76] Significantly, when aryl groups are directly attached to the *meso*-carbon, the steric hindrance favors torsional angles of

(73) Wang, Z. Q.; Day, P. N.; Pachter, R. *J. Chem. Phys.* **1998**, *108*, 2504.

(74) Kalish, H.; Camp, J. E.; Stępień, M.; Latos-Grażyński, L.; Olmstead, M. M.; Balch, A. L. *Inorg. Chem.* **2002**, *41*, 989.

(75) Holten, D.; Bocian, D. F.; Lindsey, J. S. *Acc. Chem. Res.* **2002**, *35*, 57.

(76) LeCours, S. M.; Philips, C. M.; de Paula, J. C.; Therien, M. J. *J. Am. Chem. Soc.* **1997**, *119*, 12578.

around 71°, which decreases the conjugation between the porphyrin and aryl systems.[31]

The isotropic shifts of the resonances of the capping fragments, i.e., −H and phenyl, were analyzed in detail for the high-spin iron(III) ethynylporphyrins (ETrTP)$Fe^{III}Cl$ (**1**-FeCl), (PETrTP)$Fe^{III}Cl$ (**2**-FeCl), (PBTrTP)$Fe^{III}Cl$, (**3**-FeCl), and (TrPP)$Fe^{III}Cl$ (**6**-FeCl) and the low-spin iron(III) ethynylporphyrins [(ETrTP)$Fe^{III}(CN)_2$] [**1**-Fe$(CN)_2$], [(PETrTP)-$Fe^{III}(CN)_2$][**2**-Fe$(CN)_2$], [(PBTrTP)$Fe^{III}(CN)_2$] [**3**-Fe$(CN)_2$], and [(TrPP)$Fe^{III}(CN)_2$] [**6**-Fe$(CN)_2$]. The *meso*-aryl resonances of the analyzed species are included in the comparison as well, as they represent the extent of delocalization into aryls groups directly linked to the *meso*-carbon, allowed because the aryl and porphyrinic moieties are not orthogonal.

The typical spin delocalization pathways for high-spin iron(III) porphyrins produce resonances for the β-pyrrole [(TPP)$Fe^{III}X$] or α-CH_2 [(OEP)$Fe^{III}Cl$] protons that are strongly shifted downfield. This downfield shift is a result of the σ contact contribution due to delocalization through the σ framework by way of the σ donation to the half-occupied $d_{x^2-y^2}$ iron(III) orbital. Additionally, π delocalization places a considerable amount of positive spin density at the meso positions. The mechanism has been identified as iron-to-porphyrin π back-bonding and involves the empty 4e(π^*) orbitals of the porphyrin with a large contribution from the $2p_z$ *meso*-carbon atomic orbitals.[1] We have noticed previously that the contact shift of high-spin iron(III) tetraphenylporphyrins might result from simultaneous delocalization in the σ orbitals as well as in both filled 3e(π) and vacant 4e(π^*) molecular orbitals.[7] Recently, Cheng and co-workers considered that an unpaired electron in the d_{z^2} orbital of the metal can interact with the a_{2u}-type π orbital of the macrocycle to cause significant π-spin delocalization to *meso*-carbons and that this is the major contribution to the large negative chemical shifts of the *meso*-H of chloroiron(III) octaethylporphyrin and other porphyrins.[77] The π-spin density localized at *meso*-carbons produces the sign alternation of the contact shifts measured for the *meso*-phenyl resonances in (TPP)$Fe^{III}X$ and (5-X-TPP)$Fe^{III}X$.[1,7,58] It is reflected by the large upfield shift of the *meso*-protons of (OEP)$Fe^{III}Cl$ and (5-X-OEP)$Fe^{III}Cl$.[1,74] Consequently, the high-spin five-coordinate iron(III) porphyrins are characterized by a relatively large positive spin density at the *meso*-carbon, as illustrated here by the resulting upfield localization of the *meso*-H of (TrPP)$Fe^{III}Cl$, −72.4 ppm (293 K). The positive spin density localized at the *meso*-carbon can be readily delocalized along the ethynyl or butadiyne fragment of appropriate iron(III) ethynylporphyrins. The efficiency of the spin transfer is remarkable, as illustrated by the chemical shifts of C_{meso}−**H** and −CC−**H** determined for **1**-FeCl and **6**-FeCl (Figure 4, Table 1). Substitution of the ethynyl hydrogen −CC−**H** by phenyl −CC−$\mathbf{C_6H_5}$ affords a spectroscopic pattern consistent with the π-spin density distribution around the introduced phenyl ring. Significantly, the contact shift values are comparable to those determined for *meso*-aryls of (TPP)$Fe^{III}Cl$.[61,78,79] In terms of the present considerations, chloroiron(III) 5-(phenylbutadiynyl)-10,15,-20-tri(*p*-tolyl)porphyrin (**3**-FeCl) reveals the effect of an elongation of the conducting rod by addition of one more ethynyl moiety. The comparison of the chemical shifts in the Table 1 leads to the conclusion that spin delocalization via the *meso*-butadiynyl to the capping phenyl is still operating but the effect is clearly diminished as compared to that of the phenylethynyl of **2**-FeCl. Significantly, the sign alternation around the phenyl moiety of **3**-FeCl is still detectable.

As a final point, the communication between two high-spin iron(III) porphyrinic fragments linked via the butadiyne moiety can be addressed. The similarity of the spectrum of the diiron complex **5**-$(FeCl)_2$ to those containing the analogous (TrTP)$Fe^{III}Cl$ subunit allowed us to conclude that the spin density transfer is relatively small and comparable to that via the identical linker seen for capping phenyl of **3**-FeCl.

Spin delocalization along the ethynyl substituents was observed for the low-spin complexes. Characteristic features of the spin delocalization for this particular spin state have to be considered. Thus, low-spin Fe(III) complexes of 4-fold-symmetric porphyrins such as $(TPP)H_2$ and $(OEP)H_2$ can exist in two different electronic states: $(d_{xy})^2(d_{xz},d_{yz})^3$ and the less common $(d_{xz},d_{yz})^4(d_{xy})^1$.[1] However, an increasing number of examples of the less common, $(d_{xz},d_{yz})^4(d_{xy})^1$ state have come to light recently.[1,14,17,70,80,81] For the lower-symmetry complexes $[(5\text{-R}-\text{OEP})Fe^{III}(CN)_2]^-$ where one meso position is unique, the situation is more complex, and the ground state of [(5-R−OEP)$Fe^{III}(CN)_2$] combines the features of both ground states with the composition for any one complex controlled by the nature of the *meso*-R substituent.[74]

The upfield *meso*-proton shift seen for iron porphyrins with the $(d_{xz},d_{yz})^4(d_{xy})^1$ ground state arises from the presence of spin in the a_{2u}-like porphyrin orbital, which has principal contributions at the meso positions and little or no contribution at the pyrrole positions.[1,82,83] Complexes with the $(d_{xz},d_{yz})^4(d_{xy})^1$ electronic state that involve $(OEP)^{2-}$ as the ligand are rare, but $[(OEP)Fe^{III}(t\text{-BuNC})_2]^+$ is one example that is reported to have a nearly pure $(d_{xz},d_{yz})^4(d_{xy})^1$ electronic ground state.[84] The ^1H NMR spectrum of $[(OEP)Fe^{III}(t\text{-BuNC})_2]^+$ shows that the *meso*-protons are shifted relatively far upfield ($\delta = -37$ ppm at 303 K).[84] Significantly, the positive π spin density is expected for low-spin iron(III)

(77) Cheng, R.-J.; Chen, P.-Y.; Lovell, T.; Liu, T.; Noodleman, L.; Case, D. A. *J. Am. Chem. Soc.* **2003**, *125*, 6774.
(78) La Mar, G. N.; Walker, F. A. *J. Am. Chem. Soc.* **1973**, *95*, 6950.
(79) Behere, D. V.; Birdy, R.; Mitra, S. *Inorg. Chem.* **1982**, *21*, 386.
(80) Simmoneaux, G.; Bondon, A. Isocyanides and Phosphines as Axial Ligands in Heme Proteins and Iron Porphyrin Models. In *The Porphyrin Handbook*; Kadish, K. M., Smith, K. M., Guilard, R., Eds.; Academic Press: San Diego, CA, 2000; pp 299−322.
(81) Ikeue, T.; Ohgo, Y.; Saitoh, T.; Yamaguchi, T.; Nakamura, M. *Inorg. Chem.* **2001**, *40*, 3423.
(82) Walker, F. A.; Nasri, H.; TurowskaTyrk, I.; Mohanrao, K.; Watson, C. T.; Shokhirev, N. V.; Debrunner, P. G.; Scheidt, W. R. *J. Am. Chem. Soc.* **1996**, *118*, 12109.
(83) Ikeue, T.; Ohgo, Y.; Saitoh, T.; Nakamura, M.; Fujii, H.; Yokoyama, M. *J. Am. Chem. Soc.* **2000**, *122*, 4068.
(84) Guillemot, M.; Simonneaux, G. *J. Chem. Soc., Chem. Commun.* **1995**, 2093.

porphyrins where the $(d_{xz},d_{yz})^4(d_{xy})^1$ electronic state contribute to the electronic structure, which is the case for the bis-cyanide complexes **1**-Fe(CN)$_2$, **2**-Fe(CN)$_2$, **3**-Fe(CN)$_2$, **5**-[Fe(CN)$_2$]$_2$, and **6**-Fe(CN)$_2$ formed in methanol solution. The efficiency of the spin transfer is remarkable, as illustrated by the relevant isotropic shifts for **1**-Fe(CN)$_2$ (−CC−**H**, −10.4 ppm) and **6**-Fe(CN)$_2$ (C_{meso}−**H**, −17.1 ppm). Significantly, the butadiynyl linker of **3**-Fe(CN)$_2$ transmits a sufficient amount of spin density for a measurable effect to be detected at the capping phenyl moiety.

The differences in values of the induced contact shifts can be readily explained. Specifically, different amounts of positive π spin density are originally located at the meso positions of high-spin and low-spin complexes because of the obvious differences in the nature of the ground electronic states.

In regard to the delocalization of the spin density at the phenylethynyl fragment, it is illustrative to consider the case where the phenylethynyl moiety is directly coordinated to high- or low-spin iron(III) porphyrins: (TPP)Fe^{III}(CCPh) (*o*-H, −83.9; *m*-H, 48.9; *p*-H, −77.8), (THF)(TPP)Fe^{III}(CCPh) (*o*-H, −15.6; *m*-H, 31.8; *p*-H, −19.4), (py)(TPP)Fe^{III}(CCPh) (*o*-H, −31.9; *m*-H, 32.9; *p*-H, −13.8) (chemical shift values at 203 K given in ppm in parentheses).[85] The patterns of resonances for the axial aryl protons are similar for high-spin and low spin species, as with the *ortho*- and *para*-phenyl resonances shifted upfield and *meta*-phenyl resonances shifted downfield. This pattern of shifts reflects the presence of the unpaired π spin density on the aryl groups in both cases provided by either low-spin or high-spin iron(III). The coordination is definitely the most efficient in providing the considerable amount spin density to the phenylethynyl fragment. Accordingly, an effect seemingly of the same nature is more pronounced for (TPP)Fe^{III}(**CCPh**) than for (TrTP-**CCPh**)Fe^{III}Cl (**2**-FeCl). In light of these studies, the spin density transfer documented here for the ethynyl and butadiynyl linkers is expected to be operating in the transfer of spin density by higher conjugated polyynes with end groups containing paramagnetic metals.[86]

Experimental Section

Materials. 5-Ethynyl-10,15,20-tri(*p*-tolyl)porphyrin [(ETrTP)-H$_2$, **1**], 5-(phenylethynyl)-10,15,20-tri(*p*-tolyl)porphyrin [(PETrTP)-H$_2$, **2**], 5-(phenylbutadiynyl)-10,15,20-tri(*p*-tolyl)porphyrin [(PBTrTP)-H$_2$, **3**], 5,10,15,20-tetra(phenylethynyl)porphyrin [(TPEP)H$_2$, **4**], 1,4-bis-[10,15,20-tri(*p*-tolyl)porphyrin-5-yl]-1,3-butadiyne {[(TrTP)H$_2$]$_2$B, **5**} were synthesized using known procedures.[31,32,36,47,48]

High-Spin Iron(III) Ethynylporphyrins. A solution of 500 mg of iron(II) chloride tetrahydrate (2.5 mmol) in 10 mL of methanol was added in three portions over the course of 1 h (at 20-min intervals) to a refluxing solution of the appropriate ethynylporphyrin (0.025 mmol of **1**, **2**, **3**, or **5**) dissolved in 20 mL of chloroform. After the solvent had been removed under reduced pressure, the solid residue was extracted with dichloromethane and filtered off. In the case of **4**-FeCl, **4** and a metal source were refluxed in pyridine solution for 1 h, and workup was performed using the procedure described above. Conversion into the iron(III) complexes proceeded quantitatively.

Table 3. Crystal Data for [(TPEP)H$_4^{2+}$](CF$_3$COO)$_2$·(CF$_3$COOH)$_{2.73}$·(CH$_2$Cl$_2$)$_{0.27}$ and [(TrTP)Zn(THF)]$_2$B with Refinement Details

	[(TPEP)H$_4^{2+}$](CF$_3$COO)$_2$·(CF$_3$COOH)$_{2.73}$·(CH$_2$Cl$_2$)$_{0.27}$	[(TrTP)Zn(THF)]$_2$B
emp formula	$C_{61.73}H_{35.27}N_4O_{9.46}F_{14.20}Cl_{0.54}$	$C_{94}H_{74}N_8O_2Zn_2$
fw	1273.27	1478.35
cryst syst	triclinic	monoclinic
space group	$P\bar{1}$	$P2_1/n$
a, Å	10.454(2)	15.092(3)
b, Å	14.450(4)	13.529(3)
c, Å	20.164(4)	18.244(3)
α, deg	95.81(3)	90
β, deg	97.36(3)	104.54(3)
γ, deg	110.75(3)	90
V, Å^3	2789.4(11)	3605.7(12)
T, K	100(2)	100(2)
Z	2	2
D_{calcd}, g·cm^{-3}	1.516	1.362
radiation *λ*, Å	0.71073	0.71073
μ, mm^{-1}	0.159	0.725
R1[a]	0.0577	0.0575
wR2[a]	0.1685	0.1539

[a] $R1 = \sum||F_o| - |F_c||/\sum|F_o|$, $wR2 = [\sum[w(F_o^2 - F_c^2)^2/\sum[w(F_o^2)^2]]^{1/2}$.

X-ray Data Collection and Refinement. Crystals of [(TPEP)-H$_4^{2+}$](CF$_3$COO)$_2$(CF$_3$COOH)$_{2.73}$(CH$_2$Cl$_2$)$_{0.27}$ were prepared by diffusion of methanol into a dichloromethane solution with a trace amount of TFAH contained in a thin tube. Crystals of [(TrTP)Zn-(THF)]$_2$B were obtained by diffusion of THF into a dichloromethane solution of **5**-Zn$_2$. Crystal data for both compounds are given in Table 3, together with refinement details. The crystals were mounted on glass fibers and then flash-frozen to 100 K (Oxford Cryosystem-Cryostream Cooler). Preliminary examination and intensity data collections were carried out on an Oxford Diffraction KM4CCD *κ*-axis diffractometer with graphite-monochromated Mo Kα radiation. The data were corrected for Lorentz and polarization effects. For [(TrTP)Zn(THF)]$_2$B crystals, an analytical absorption correction was applied.[87] Data reduction and analysis were carried out with the Oxford Diffraction (Wrocław) programs. The structures were solved by direct methods (program SHELXS97)[88] and refined by the full-matrix least-squares method on all F^2 data using the SHELXL97 programs.[89]

In the cell unit of [(TPEP)H$_4^{2+}$](CF$_3$COO)$_2$(CF$_3$COOH)$_{2.73}$·(CH$_2$-Cl$_2$)$_{0.27}$, the dichloromethane and TFAH molecule share one position with occupancies of 0.27 and 0.73, respectively. Additionally, one oxygen atom in the TFA anion and one in the TFAH molecule are disordered and occupy two positions (0.9 and 0.1 occupancy, respectively).

The center of [(TrTP)Zn(THF)]$_2$B is located at a crystallographic inversion center. [(TrTP)Zn(THF)]$_2$B (**5**-Zn$_2$) contains two disordered methyl groups. In both structures, non-hydrogen atoms were refined with anisotropic displacement parameters except disordered atoms. The hydrogen atoms of *p*-methyl groups of [(TrTP)Zn-(THF)]$_2$B and the dichloromethane molecule in the (TPEP)H$_4^{2+}$ crystal were included in the calculated positions and refined using a riding model.

(85) Balch, A. L.; Latos-Grażyński, L.; Noll, B. C.; Phillips, S. L. *Inorg. Chem.* **1993**, *32*, 1124.
(86) Szafert, S.; Gladysz, J. A. *Chem. Rev.* **2003**, *103*, 4175.
(87) KM4 CCD Software: *CrysAlis CCD* and *CrysAlis RED*, version 1.171; Oxford Diffraction Poland: Wrocław, Poland, 2003.
(88) Sheldrick, G. M. *SHELXS97: Program for Crystal Structure Solution*; University of Göttingen: Göttingen, Germany, 1997.
(89) Sheldrick, G. M. *SHELXL97: Program for Crystal Structure Refinement*; University of Göttingen: Göttingen, Germany, 1997.

Instrumentation. NMR spectra were recorded on a 500 MHz Bruker Avance spectrometer equipped with a broadband inverse gradient probehead. Proton data are referenced to the residual solvent signals. Mass spectrum of **5**-$(FeOFe)_2$ was recorded on the Voyager-Elite Spectrometer (CBMiM, Łódź, Poland) using the MALDI-TOF technique.

Acknowledgment. This work was supported by the Ministry of Scientific Research and Information Technology of Poland (KBN) under Grant 3 T09A 162 28.

Supporting Information Available: Crystallographic data in CIF format. VT NMR data for **1**-FeCl, **2**-FeCl, **3**-FeCl, **4**-FeCl, and **5**-$(FeCl)_2$. ^{1}H NMR parameters for zinc(II) ethynylporphyrins, low-spin iron(III) ethynylporphyrins in methanol-d_4 saturated with KCN and low-spin iron(III) ethynylporphyrins obtained by addition of (TBA)CN to chloroform-*d* solution. This material is available free of charge via the Internet at http://pubs.acs.org.

IC050158Q